A Study of Stability Analysis for Slopes

By Shoji OGINO*, Yoshiaki MIZUTA*
and Sunao KUNIMATSU**

(Received July 14, 1977)

Abstract

In order to investigate the analysis methods for slope stability, stress analysis using finite element method and model experiment using barodynamics equipment were performed for four different models. Slip lines were determined using stress trajectories obtained by the stress analysis and results of triaxial test on material of the model. Magnitude of centrifugal acceleration at which failure of the slope occur was determined theoretically and compared with results of experiment. With regard to models used in this study, failure of the slope always initiates at the lower end of the slope, and a approximately triangular zone up to central part of the slope slides. Such mode of failure greatly differs from the failure on a circular arc which is so far generally assumed in slope stability analysis.

Introduction

Since large scale open-pit excavations have been carried out at various mines and quarries in recent years, security of slope stability has come to one of important technical problems in mines and quarries. Many analysis methods for slope stability have hitherto been proposed, and analysis of stresses and deformations using finite element method[1)2)3)] or model experiment by means of barodynamics apparatus have been carried out of late years[4)5)6)].

Most analysis methods for slope stability which have been generally used for a long time are based on comparison of resultant force of shear stresses produced along an imaginary slip plane by weight of ground above the plane with resistive force along this plane. However, since collapse of a slope is caused by stresses due to gravity, and these stresses can be obtained by analysis, it is thought to be more reasonable to determine the slip plane based on stress analysis, giving the real state of the stresses as conscientiously as possible, than to draw an imaginary line.

From such point of view, the authors firstly made analysis of the stresses in the ground which constitute the slope under uniform gravitational force using the finite element method, and then investigated the conditions for fracture initiation in a model of slope by means of the barodynamics experiment in which the slope models are stressed in a field of centrifugal force. Stresses produced in a model by the centrifugal force in barodynamics experiment were analyzed as well. Conditions for fracture initiation in a slope were also investigated theoretically using the results of the stress analyses

* Department of Mining and Mineral Engineering
** Graduate Student, Mining and Mineral Engineering

for the model as well as results of triaxial test on material of the model.

2. Analysis of Stress in Slope

Analysis of stress in a slope under field of gravity

Analysis of stress in a state of plane strain induced by gravity in a ground which constitute a slope was carried out using finite element method, assuming that the ground is homogeneous isotropic elastic body. Results of the analysis are not described here, since they are similar to those which have hitherto been presented.

Analysis of stress in a slope model under field of centrifugal force

Analysis of stress in a slope model which is subjected to centrifugal force by barodynamics experiment was carried out as well. In the barodynamics experiment a rotation frame, in both ends of which two models are mounted, is rotated, and centrifugal acceleration, which is proportional to square of revolution speed of the rotation frame, is induced in the model. When the centrifugal acceleration is equal to λ times of acceleration of gravity, stress and strain at any point in the model are equal to stress and strain induced by gravity, at a corresponding point in a prototype which has dimensions λ times as large as that of the model, and consists of the same material as the model, provided that r, distance from rotation axis to the model, is large enough as compared with dimensions of the model[6]. Hence the revolution rate $n(s^{-1})$ which induces stress and strain at any point in the model equal to these at a corresponding point in a prototype, consists of the same material as the model, is given by

$$n=\sqrt{\lambda g/r}\,/2\pi \qquad \cdots\cdots\cdots(1)$$

where g is acceleration of gravity. Distribution of stresses and deformations in a model and a prototype are similar at any revolution speed.

When the distance from the rotation axis to the model is not large enough as compared with dimensions of the model, distribution of stresses and deformations in a model and a prototype are not similar, because acceleration of centrifugal force increases in proportion to the distance from the rotation axis. Stresses induced in the model which is subjected to centrifugal force were analyzed, therefore, taking variation of centrifugal accelaration with the distance from the rotation axis, and the extent of collapse as well as revolution speed at which collapse of the model initiates was determined using the results of the stress analysis. This revolution speed theoretically obtained was then compared with revolution speed at which collapse in model initiates determined by the barodynamics experiment.

In the analysis of stress in the slope model induced by the centrifugal force, weight per unit volume γ of any triangular element constituting analysis model are shown in Fig. 1, for an example, was determined, taking the variation of the acceleration of centrifugal force with the distance from the rotation axis into account, by the following equation:

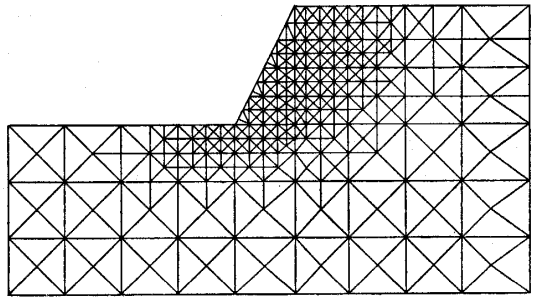

Fig. 1 Finite-element model of slope with gradient tan $\theta=2$.

$$\gamma=\rho\alpha(r_1-a)/r_1 \qquad \cdots\cdots\cdots(2)$$

where r_1 is distance between rotation axis and bottom of the model, a is height of center of gravity of any triangular element from bottom of the model, ρ is density of material of the model and α is centrifugal acceleration at the bottom of the model. Grav-

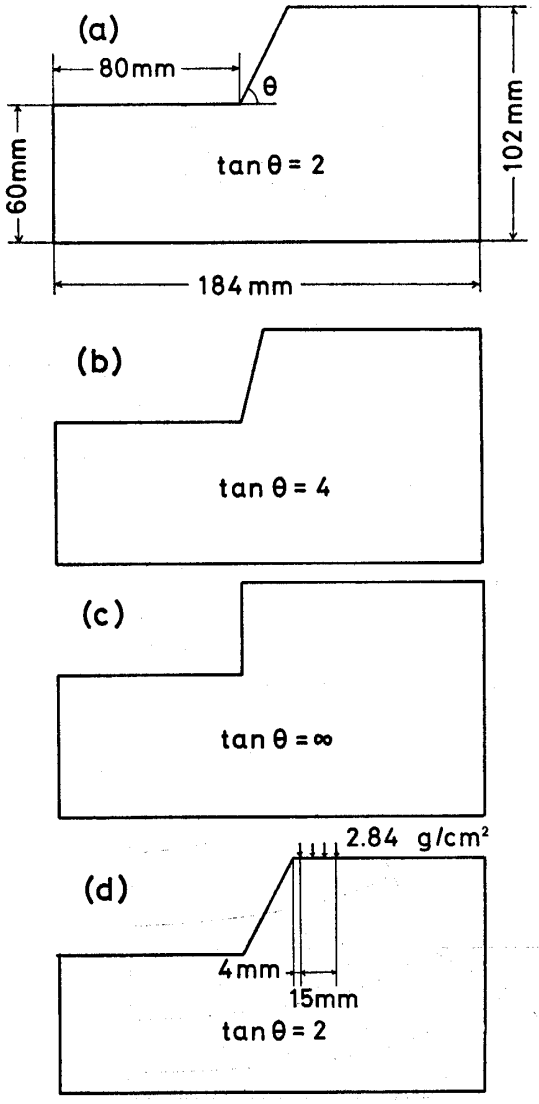

Fig. 2 Slope models.

itational acceleration acting perpendicular to centrifugal force was neglected, because its value is low enough as compared with the centrifugal acceleration.

Stress analysis mentioned above was carried out for four cases, corresponding to conditions in the experiment as shown in Fig. 2(a), (b), (c) and (d), in which shape of the model or loading conditions are different. Three inclination angles were chosen so that $\tan\theta=2$, 4 and ∞. Stress analysis as well as experiment were also carried out for a model as shown in Fig. 2(c), in which $\tan\theta=2$ and uniformly distributed load 2.84 g/cm^2 exists on the upper horizontal surface. Fig. 3 shows magnitudes and directions of principal stresses at the center of gravity of each elements in the proximity of slope obtained by the stress analysis for a model shown in Fig. 2, in which gradient of the slope $\tan\theta=2$. Every stress in this case is compressive, and half length of two segments of the crossing lines indicates the ratio of principal stress to γh_1, where h_1 is height of the upper horizontal surface from the lower horizontal surface. Stress trajectory for a model in which $\tan\theta=2$ is shown in Fig. 4.

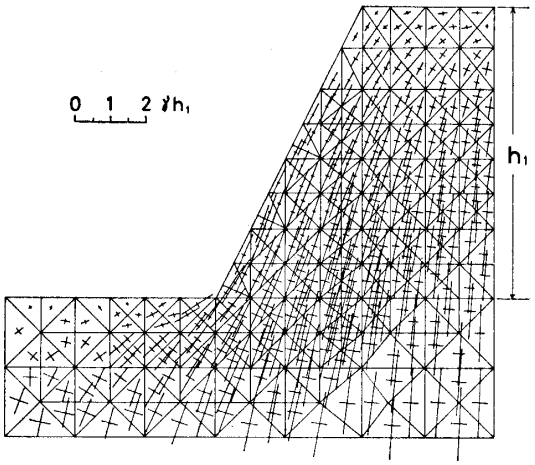

Fig. 3 Magnitude and direction of principal stresses in a slope with gradient $\tan\theta=2$.

Since concentration of stress occurs at the lower end of the slope as shown in Fig. 3, it is thought that this portion is most liable to fail. Result of stress analysis for a

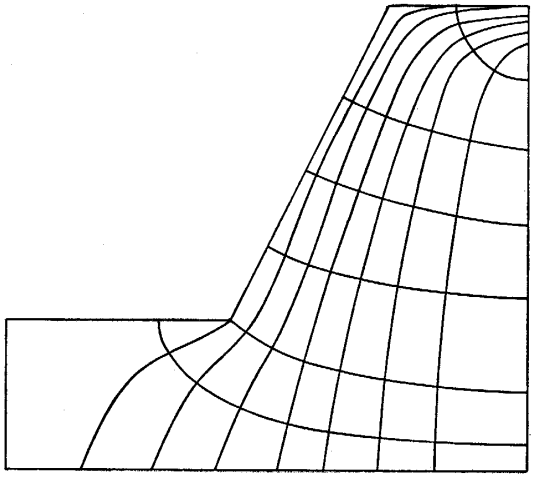

Fig. 4 Stress trajectory in a slope model with gradient $\tan\theta=2$.

model having vertical slope shows that a tensile region appears near the upper horizontal surface. However, failure may not occur in this region, because the values of the tensile stresses are very small.

Stability Analysis based on the Results of Stress Analysis

Magnitudes and directions of the principal stresses were obtained by the stress analysis mentioned above. It is thought that collapse of ground constituting the slope may occur along slip planes within the region in which state of stresses that satisfy the condition of failure. It is supposed that these slip lines have inclination $\pm(\pi/4-\phi/2)$ with direction of the maximum compressive stress, where ϕ is angle of internal friction of the material. Slip lines were determined from the point of view mentioned above, using the value of internal friction of the material which was determined by the triaxial tests and the stress trajectory as shown in Fig. 4. Fig. 5 shows slip lines for a model in which gradient of slope $\tan\theta=2$.

Five slip lines along which slip may be most liable to occur were chosen, taking results of the model experiments into account. Then, failure conditions for each of four approximately triangular zones which are surrounded by two slip lines and surface of slope, as shown in Fig. 6(a), (b), (c) and (d) by hatching were determined. In Fig. 7, intersecting point of two normals of slip lines AB and BC at the upper and lower ends of the hatched zone is represented by O. Denoting the moment around O exerted by forces acting on slip lines AB and BC so that slip failure is induced on these lines by M_1, and the moment around O exerted by resistive forces on these lines by M_2, slip failure may occur when M_1 is equal to M_2.

For actual slope being subjected to gravity, M_1 and M_2 are given by

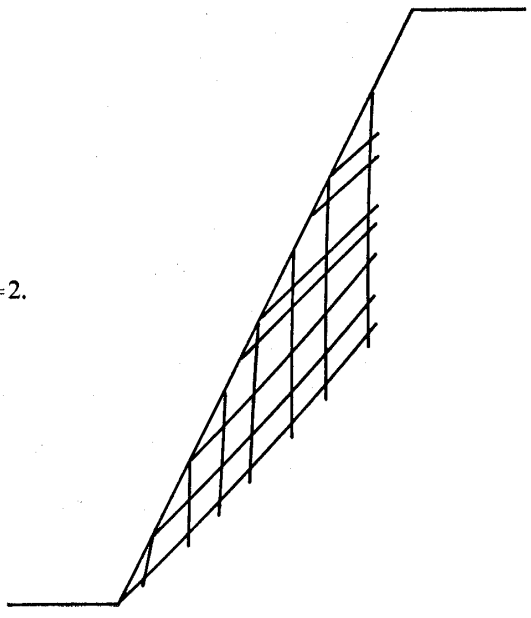

Fig. 5 Slip lines in a slope with gradient $\tan\theta=2$.

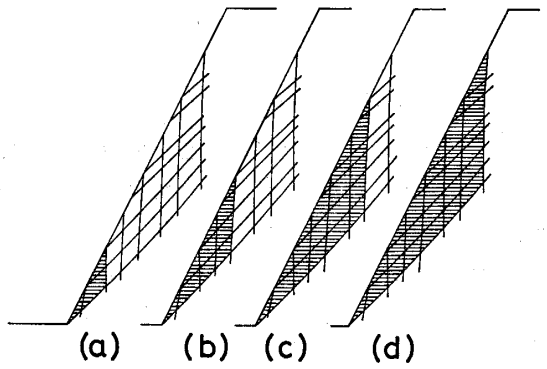

Fig. 6 Slip zones surrounded by two slip lines and slope surface (hatched zone).

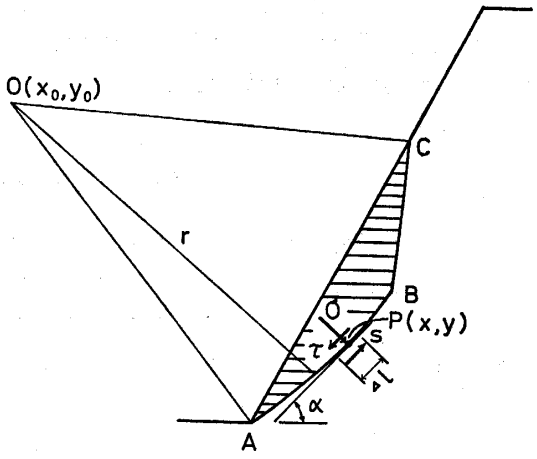

Fig. 7 Slope stability analysis for a slip zone.

$$M_1=\Sigma\bar{r}\tau\Delta l \qquad \cdots\cdots(2)$$

$$M_2=\Sigma\bar{r}s\Delta l \qquad \cdots\cdots(3)$$

where τ and s are the shear stress and resistive force on an element of the slip lines Δl at point P, and $\bar{r}$ is distance from point O to tangent of the slip line at point P. s is given by

$$s=c-\sigma\tan\phi \qquad \cdots\cdots(4)$$

where σ is normal stress across the slip line at point P. c and ϕ are cohesion and angle of internal friction of the material. Sign of σ was chosen so that positive σ represents tensile stress.

For slope model being subjected to gravity, equations (2), (3) and (4) are still applicable for any point P on slip lines in this model. When this model is subjected to centrifugal force, the values of the stresses in the model increase. Shear stress τ' and the resistive force s' at a corresponding point are given by

$$\tau'=\lambda\tau$$

$$s'=\lambda s-(\lambda-1)c$$

where λ is the ratio of centrifugal acceleration at this point to acceleration of gravity. Denoting the moment around O exerted by forces acting on the slip lines in the model by which slip failure is induced on these lines by M_1', and the moment around O exerted by resistive forces on these lines by M_2', M_1' and M_2' are given by

$$M_1'=\lambda\Sigma\bar{r}\tau\Delta l=\lambda M_1$$

$$M_2'=\Sigma\bar{r}\{\lambda s-(\lambda-1)c\}\Delta l$$

$$=\lambda M_2-(\lambda-1)k$$

where $k=c\Sigma\bar{r}\Delta l$.

Accordingly λ, ratio of the centrifugal acceleration to the gravitational acceleration g, by which collapse of the slope initiates, is given by

$$\lambda = k/(M_1 - M_2 + k). \qquad \cdots\cdots(5)$$

When the slip line is a segment of straight line or circular arc, λ is given by

$$\lambda = c\Sigma\Delta l/(\Sigma c\Delta l - \Sigma s\Delta l + c\Sigma\Delta l). \qquad \cdots\cdots(6)$$

Safety factor of the slope is

$$F = M_2'/M_1' = \{\lambda M_2 - (\lambda - 1)k\}/\lambda M_1. \qquad \cdots\cdots(7)$$

Collapse of the slope initiates at $F=1$. Safety factor for any value of λ is given by equation (7). Equations (5), (6) and (7) can be applied to determine the dimension ratio of prototype to model made of same material as well as safety factor.

In calculation of values M_1 and M_2 by equations (1) and (2), Δl was taken as segment length of slip line in a triangular element, and $\bar{r}$ was determined by

$$\bar{r} = (x - x_0)\sin\alpha + (y - y_0)\cos\alpha$$

where x, y are coordinates of point P, x_0, y_0 are coordinates of point O and α is slope of tangent to x-direction.

Triaxial compression test on material of the model in order to determine the values of c and ϕ was carried out using triaxial apparatus type 18IS manufactured by Kyushu-Maruto. Fig. 8 shows Mohr's circles and a envelop obtained by this test, from which values $c=0.925$ kg/cm^2 and $\phi=24.5°$ were determined.

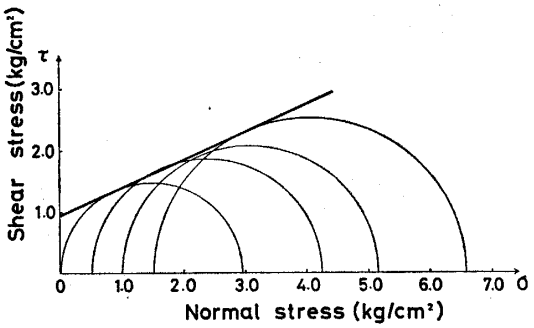

Fig. 8 Results of triaxial test for the material of model.

Dimension ratio of prototype to model, at which collapse by gravity occurs in the prototype, was determined for the model with slope gradient $\tan\theta=2$, assuming that materials of prototype and model are same. Values of the ratio λ are shown in Fig. 9. These λ values represent the ratio of actual hight at which collapse of the hatched zone occurs, to that of model. Since the height of the slope is 40 mm, height H of actual slope can be obtained as shown in Fig. 9.

Values of λ which cause collapse of triangular zone surrounded by slip lines and slope surface were calculated by the procedure mentioned above for all models shown

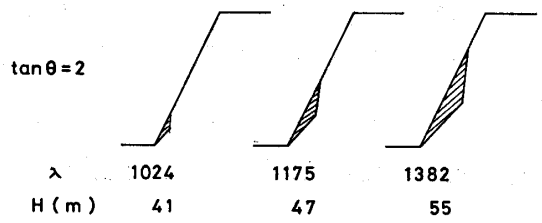

Fig. 9 Dimension ratio λ of actual slope to the model and height of the actual slope H, at which slip of hatched zone occur.

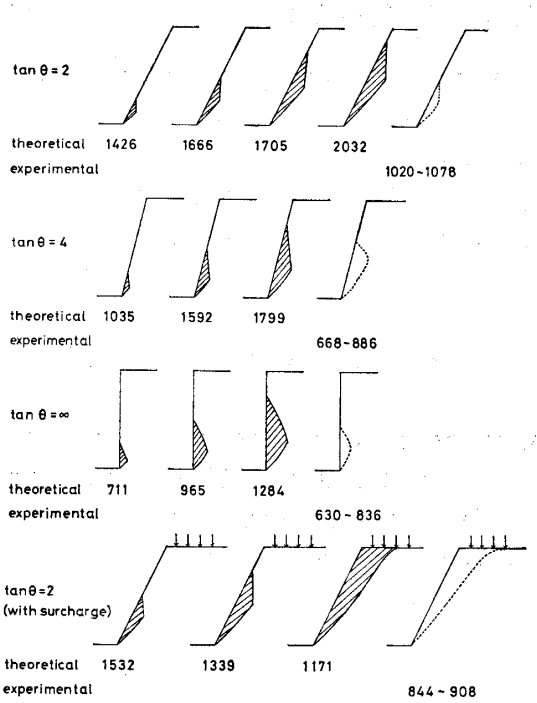

Fig. 10 Values of λ at which slip of the hatched zone occurs.

in Fig. 2. Results of this calculation are shown in Fig. 10. Figures shown in the line of "theoretical" indicate the values of λ at which hatched zone in the illustration over the figure breaks.

Model Experiment

Experimental Apparatus

A barodynamics equipment, which was constructed by Mikumo, Hiramatsu and Fujinaka, was used for slope model experiment, applying partial reform. Slope models are mounted on both ends of the rotation frame as shown in Fig. 11, so that bottom and side planes of the model become vertical. Distance from rotation axis to the bottom is 212 mm.

The driving unit for the centrifuge is Ward Leonard system which consists of a 3 phase 5 HP induction motor, a DC 5 HP generator, DC 3 HP mortor and a control

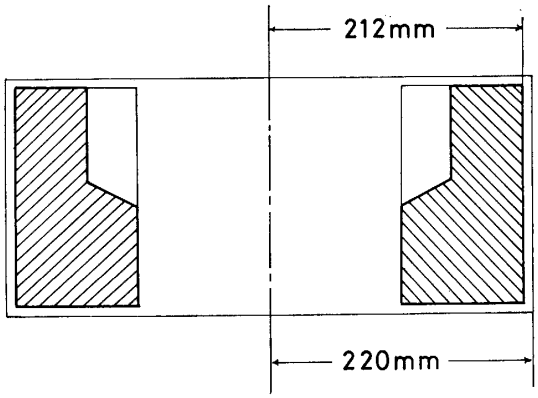

Fig. 11 Position of models in the rotating frame.

unit. Revolution speed of the centrifuge is controlled smoothly by this system from creep speed up to 3400 rpm.

The revolution speed was measured by photo-tachometer of type PT–300 made by Sugahara Kenkyusho which works by reflection beam from small mirror attached on the revolving shaft of the centrifuge. Electric conductive paint was painted on the center line of slope, upper and lower surfaces of two models mounted on both ends of the rotation frame, in order to determine the revolution speed at which break of a slope occur. The electric conductive paint on each model was connected to Y_1- and Y_2-axis of XYY recorder using a slip ring of type RBE–E made by Kyowa Dengyo as shown in Fig. 12. Output of the photo-tachometer was used as input of X-axis of the recorder, and revolution speed at which each line of electric conductive paint is cut by break of the slope. Fig. 13 shows the barodynamics equipment used for this study.

Model

Model of slope was made by mixing plaster of Paris, calcium carbonate, standard sand and water in weight ratio of 1: 1: 10: 4, placing it into a mould, shaping to prescribed shape and dimensions, and drying the shaped model for 3 hours at 20°C and 24 hours at 50°C. Three types of models as shown in Fig. 2(a), (b) and (c), width of which is 90 mm, were made. The model was mounted in the rotating frame after being placed in a rectangular box made of aluminium plate. Inner dimensions of this box are equal to breadth, length and height of the model, and thickness of side plates are 3 mm. For the case in which a part of upper horizontal surface is uniformly loaded as shown in Fig. 2(d), experiment was carried out using models with $\tan\theta=2$. Solder was used for applying the uniformly distributed surcharge.

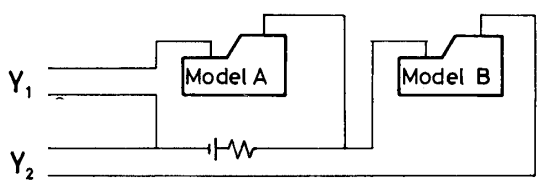

Fig. 12 Detection method of slope failure.

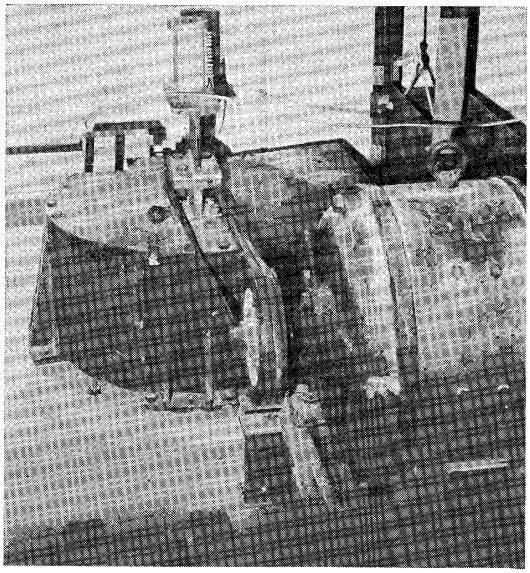

Fig. 13 Earodynamics equipment.

Results of Model Experiment

Revolution speed at which slope of a model collapse was determined, increasing the revolution speed gradually at rate of 50～100 rpm/min. Number of revolution N and ratio of centrifugal acceleration to gravitational acceleration λ at which slope of the model collapesed are shown in Table 1. By the comparison of the values of λ, in

Table 1. Number of revolution N and ratio of centrifugal acceleration on the bottom of the model to acceleration of gravity λ, at which slope failure occurs.

Model No.	Slope gradient	N (rpm)	λ	Remarks
1A	tan $\theta=2$	2036	1020	
1B		2036	1020	
2A		2093	1078	
2B		2093	1078	
3A	tan $\theta=4$	1897	886	
3B		1883	872	
4A		1648	668	
4B		1648	668	
5A	tan $\theta=\infty$	1600	630	
5B		1661	680	
6A		1750	754	
6B		1843	836	
7A	tan $\theta=2$	1921	908	uniformly distributed load exists on the upper surface
7B		1852	844	

Table 1 determined by experiment, to that in Fig. 11, determined theoretically, it can be seen that both values show sufficient conformity for models with vertical slope, while experimental value are lower than theoretical values in some degree.

Failure of the slope initiated in all models at the lower end of the slope, and then approximately triangular zone extending from the lower end to central part of the slope as shown in the right end of Fig. 10 by broken lines collapsed. If the revolution speed is increased after the failure, cracks being due to tensile stress arize in the upper horizontal surface, and the secondary collapse comes up to upper part of the slope. Such mode of failure greatly differs from the failure on a circular arc which is hitherto generally assumed in slope stability analysis. Fig. 14 shows the primary failure which occured in the slope with gradient $\tan\theta=2$.

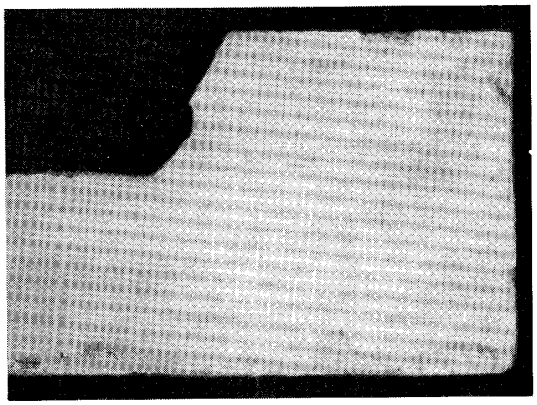

Fig. 14 Primary failure which occured in the slope with gradient $\tan\theta=2$.

In the case in which the uniformly distributed load is exerted on the upper horizontal surface, failure occured approximately along a line which connects lower end of the slope and end of the surcharge opposite to the slope. Fluctuation in λ values in Table 1 may be due to the degree of lateral confinement by the aluminium box.

Summary and Conclusions

In order to investigate the analysis methods for slope stability, in which inclination of the slope is fairly steep and the ground constituting the slope is continous body consists of brittle material as in the case of open-pit slopes, stress analysis using finite element method and model experiment by barodynamics equipment, for four cases in which shape or loading conditions are different, were carried out.

First, stresses in the ground which constitute the slope under gravity were analyzed. Secondly, stresses in a slope model under centrifugal force exerted by rotation of the centrifuge were analyzed, taking the increase of centrifugal acceleration with the distance from rotation axis into account. Slip line nets were determined, using stress trajectories obtained by the analysis and value of internal friction angle determined by triaxial test. Theoretical consideration was performed, then, in order to determine the revolution speed at which collapse of approximately triangular zone surrounded

by two slip lines, along which collapse of material most liable to take place, and slope surface occurs, taking magnitudes of stresses obtained by the analysis and results of triaxial test of the material into account. This revolution speed was compared with that obtained by model experiment at which collapse of the slope take place. Following conclusions were obtained from the analyses and the model experiments:

(1) With regard to slope models used in this study, failure of the slope always intitiates at the lower end of the slope, and an approximately triangular zone up to central part of the slope slides. Results of the model experiment and results obtained by the slope stability analysis using the results of stress analysis and triaxial test of the material showed approximately tolerable conformity. Secondary collapse takes place after the primary collapse mentioned above occurs, by tensile stresses which arize in the upper horizontal surface.

(2) Although circular arc is generally assumed so far in the slope stability analysis, this assumption is not thought to be adequate within range of the stress analysis and the model experiment in this study. It is thought to be reasonable to determine the slip plane not by assumption but by stress analysis.

(3) Results of the model experiment showed some difference from the results obtained theoretically using the method for slope stability analysis described in this paper. This discrepancy may be caused by insufficiency of lateral confinement of the model.

(4) Reliability of results may be improved by stability analysis based on elasto-plastic analysis taking failure criteria for three dimensional stress state into account.

References

1) Kawamoto, T. "On the State of Stress and Deformation of Natural Slopes", Rock Mechanics in Japan, **1**, 82–84 (1970).
2) Kaneshige, O., Okamura, H. and Akimoto, A. Preprint, MMIJ Spring Meeting 1976, 243–244 (in Japanese).
3) Finn, W. D. L. "Static and Dynamic Stresses in Slopes", Proc. 1st Congress of ISRM, Lisbon, **2**, 167–169 (1966).
4) Goldstein, M., Berman, M., Goosev, B., Timoteyena, T. and Turovskaya, A. "Stability Investigation of Fissured Rock Slope", Proc. 1st Congress of ISRM, Lisbon, **2**, 175–178 (1966).
5) Yamaguchi, H., Kimura, T., and Fujii, N. "Slope Stability Experiments using Centrifuged Models", Technical Report, Dpt. Civil Eng., Tokyo Inst. Technology, No. 15, 37–61 (1973).
6) Mikumo, E., Hiramatsu, Y. and Fujinaka, Y. "On the Model Tests of Underground Pressure Problems", Jour. Mining & Metal. Inst. Japan, **68**, 307–311 (1952) (in Japanese).